Available online at www.sciencedirect.com
SCIENCE DIRECT®
Journal of Solid State Chemistry 179 (2006) 56–61
JOURNAL OF SOLID STATE CHEMISTRY
www.elsevier.com/locate/jssc

Selected-control solution-phase route to multiple-dendritic and cuboidal structures of PbSe

Benxia Li, Yi Xie*, Yang Xu, Changzheng Wu, Zhengquan Li

Nanomaterials and Nanochemistry, Hefei National Laboratory for Physical Sciences at Microscale, Department of Chemistry, University of Science and Technology of China, Hefei, Anhui 230026, China

Received 8 August 2005; received in revised form 20 September 2005; accepted 24 September 2005
Available online 28 October 2005

Abstract

Well-crystalline PbSe multiple-dendritic hierarchical structures have been prepared through a facile hydrothermal process in an alkaline glycerol/water solution system using SeO_2 as selenium source and hydrous hydrazine as reducing agent at 160 °C for 12 h. The obtained products were characterized by X-ray powder diffraction, field emission scanning electron microscopy and transmission electron microscopy, which showed that the obtained products were face-centered cubic PbSe multiple-dendritic superstructures with length of each dendrite ranging from 1.0 to 1.5 μm. Additionally, cuboidal PbSe microcrystals with different concave faces can be obtained through a similar process except for using Se powders instead of SeO_2 as selenium source and without hydrous hydrazine. The edge lengths of these cuboidal microcrystals range from 1.0 to 2.5 μm observed by field emission scanning electron microscopy. The influencing factors for the formation of the two kinds of PbSe microstructures were discussed and the possible growth mechanisms were proposed from the point of crystallographic and kinetic views. The studies on the corresponding photoluminescence (PL) properties of the two kinds of PbSe structures are also carried out.

Keywords: Selected-control; Glycerol/water; Dendritic; Cuboidal; PbSe

1. Introduction

Synthesis of inorganic semiconductor nanomaterials with specific morphology has attracted considerable attention for decades due to their special properties [1,2] and they are destined to be widely applied in fabricating nanoscale electronic or electromechanical devices because the properties of semiconductor nanocrystals are strongly influenced by their sizes and shapes [3,4]. In addition, chemical synthesis of functional materials with organized arrangement is an important type of material architecture, as it resembles many natural dynamical processes in which formation and organization take place simultaneously [5]. Multiple-dendritic assemblies are one type of superstructures generally formed by hierarchical self-assembly under relevant conditions [6–8]. Inorganic semiconductors with hierarchical and repetitive dendritic superstructure in microscale have attracted a great deal of attention in recent years because of their intrinsic electronic, magnetic, photonic, and catalytic properties [9–11]. Investigation of hierarchically self-assembled patterns in chemical systems has indicated that the distinct shape and chemical functionality of such structures make them promising candidates for the design and fabrication of new functional materials [12]. Such structures can also have advantages in the generation of hierarchical nanostructured network over their counterparts of nanorods, nanowires, and nanoprisms, but it is challenging to develop simple and novel synthetic approaches for building hierarchical architectures of various systems.

There has been a growing interest in the synthesis and characterization of selenides due to their unique properties and wide applications in sensors, lasers, solar cells, infrared detectors, thermoelectric cooling materials, and so on [13–16]. PbSe is one of the most attractive selenides for a wide range of applications and is an important semiconductor owing to its small bandgap (0.27 eV) and large Bohr

*Corresponding author. Fax: +86 551 360 3987.
E-mail address: yxielab@ustc.edu.cn (Y. Xie).

0022-4596/$ - see front matter © 2005 Elsevier Inc. All rights reserved.
doi:10.1016/j.jssc.2005.09.043

exciton radius. Various synthetic methods for many different PbSe nanostructures have been reported, including microwave-assisted preparation or sonochemical methods to nanoparticles, solution-phase hydrothermal route to nanowires, and so on [17–19]. However, to the best of our knowledge, select-control synthesis of complex 3D nanostructures of PbSe such as multiple-dendritic and cuboidal structures has scarcely been reported.

In this work, PbSe multiple-dendritic hierarchical structure with 4-fold structural symmetry and cuboidal microcrystals with concave faces were selectively obtained by using different selenium sources in a glycerol/water solution system. When SeO_2 was used as selenium source and hydrous hydrazine as reducing agent in the system, multiple-dendritic PbSe microcrystals with hierarchical structures can be obtained. Additionally, using Se powders as selenium source instead of SeO_2 and in the absence of hydrous hydrazine, PbSe cuboidal microcrystals were produced.

2. Experimental section

2.1. Synthesis

All chemicals used were analytical grade. For synthesis of PbSe multiple-dendritic hierarchical structure, in a typical experiment, the starting solution was prepared by mixing 35 ml of 0.05 M $Pb(NO_3)_2$ solution dissolved in glycerol(5 ml)–H_2O(30 ml) solvent and 5 ml of 8 M NaOH solution. Then 2 mmol SeO_2 and 1.0 g SDBS (dodecyl benzene sulfonic acid sodium salt) were dissolved into the solution and 5 ml hydrous hydrazine (85% wt) was finally added. After being vigorously stirred for half an hour, the mixed solution was put into a Teflon lined autoclave of 50-ml capacity and heated at 160 °C for 12 h. Gray precipitate was obtained finally. The product was washed for several times by deionized water and pure ethanol, respectively, to remove organic remainders and inorganic ions.

For synthesis of PbSe cuboidal microcrystals, we used Se powders as selenium source instead of SeO_2 and in the absence of hydrazine. The experimental process was carried out as the synthesis of PbSe multiple-dendritic structures.

2.2. Characterization

X-ray diffraction (XRD) analyses were performed using a Japan Rigaku D/max-cA X-ray diffractometer equipped with graphite monochromatized high-intensity Cu$K\alpha$ radiation ($\lambda = 1.54178$ Å). The X-ray photoelectron spectra (XPS) were collected on an ESCALab MKII X-ray photoelectron spectrometer, using nonmonochromatized Mg$K\alpha$ X-ray as the excitation source. FESEM images were taken on a JEOL JSM-6700F SEM and transmission electron microscopy (TEM) was performed on a Hitachi (Tokyo, Japan) H-800 transmission electron microscope at an accelerating voltage of 200 kV. The room temperature photoluminescence (PL) spectra were performed on a Jobin Yvon-Labram spectrometer with a He–Cd laser.

3. Results and discussions

3.1. X-ray diffraction patterns of the products

All of the obtained products were milled in an agate mortar before they were characterized by X-ray powder diffraction. The representative XRD patterns of the PbSe multiple-dendritic and cuboidal structures are shown in Fig. 1. All the peaks in two XRD patterns can be indexed as the face-centered cubic (fcc) PbSe (JCPDS card 06-354, $a = 6.124$ Å). No characteristic peaks of impurities, such as PbO or Se, were observed, indicating the high purity of the products. In addition, the strong and sharp reflection peaks suggest that the products are highly crystalline.

3.2. The X-ray photoelectron spectra

Further evidence for the quality and composition was obtained by the XPS of the products, and the XPS spectra of two kinds of PbSe microstructures are identified. The binding energies obtained in the XPS analysis were corrected for specimen charging by referencing the C 1*s* to 284.60 eV. The higher-resolution spectra of the Pb and Se regions of PbSe microstructures are shown in Supporting Information. The strong peak observed in the Pb region at 137.7 eV is assigned to the (4*f*) Pb binding energy; the peak in the Se energy region is detected at 53.3 eV and is attributed to (3*d*) Se [19,20]. The (4*f*) Pb and (3*d*) Se peak areas quantified the content of Pb and Se and gave the atomic ratio of Pb to Se as 1:0.90, which is close to stoichiometric ratio of PbSe (1).

3.3. Morphologies of the PbSe microstructures

The morphologies of the obtained products were examined by FE-SEM (Figs. 2a–c) in which the solid

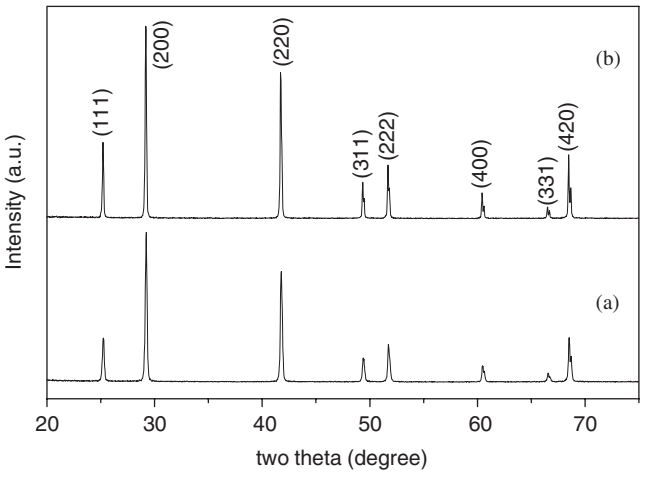

Fig. 1. XRD patterns of (a) multiple-dendritic PbSe superstructures and (b) cuboidal PbSe microcrystals.

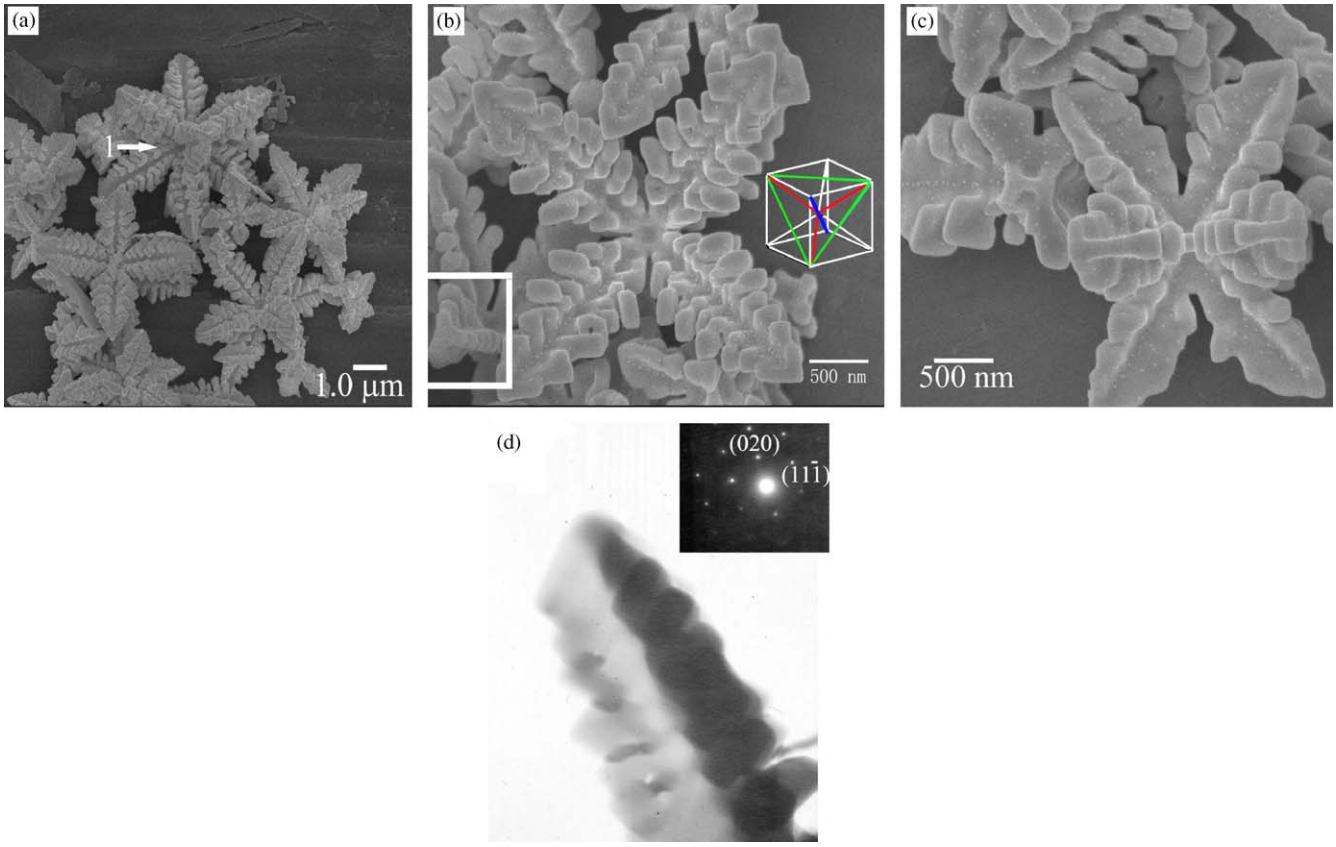

Fig. 2. SEM and TEM images of the multiple-dendritic hierarchical structures: (a) the panoramic image; (b) the obverse and (c) the side view of a typical PbSe multiple-dendritic structure; (d) TEM image of a dendritic fractal and SAED patterns recorded on it. Inset in (b) illuminates the growing directions of a dendritic fractal in PbSe multiple-dendritic hierarchical structure.

samples were mounted on copper meshes without any dispersion treatment and TEM (Fig. 2d) in which the sample was dispersed in absolute ethanol with ultrasonic treatment. Figs. 2a–d show the FESEM and TEM images of the samples prepared by the process using SeO_2 as selenium source and hydrous hydrazine as reducing agent. As shown in the panoramic image (Fig. 2a), there are many structurally 4-fold symmetrical superstructures consisting of eight dendritic offshoots. Typically, a single multiple-dendritic structure marked with arrow 1 in Fig. 2a, one dendritic offshoot of which is parallel to our line of sight, reveals the structures of the 4-fold symmetric multiple-dendritic hierarchical structure are three-dimensional (3D) eight-offshoot frameworks. Figs. 2b and c display, respectively, the obverse view and the side view of a typical PbSe multiple-dendritic structure with 4-fold structural symmetry. Close observations in Fig. 2b reveal a well-defined multiple-dendritic structure with four pronounced dendritic-shaped offshoots distributing symmetrically. In detail, observed from the image marked with a frame in Fig. 2b, individual dendritic offshoot in this structure presents 3-fold symmetrical structure, agreement with the image marked with arrow 1 in Fig. 2a, which indicates that each dendritic offshoot in the hierarchical structure has 3D structure consisting of one trunk and small branches symmetrically distributed on three sides of the trunk. The lengths of the trunks are 1.0–1.5 μm, and those of the branches range from 100 to 300 nm. The side view in Fig. 2c, two offshoots hiding from view, can further confirm the structures of the multiple-dendritic hierarchical structure are 3D eight-offshoot structures. Fig. 2d shows the TEM image of a dendritic fractal and the selected area electron diffraction (SAED) pattern (inset in Fig. 2d) taken from the dendrite, indicating that the trunk and the branches grow along the crystallographically equivalent directions of $\langle 111 \rangle$.

Figs. 3a–c show the SEM images of the sample obtained in the reaction system using Se powders as selenium source without hydrous hydrazine. Many cubes with edge lengths ranging from 1.0 to 2.5 μm are present in the sample, and the proportion of the cubes in the sample was estimated to be 60%. A panoramic image of the sample was shown in Fig. 3a, from which some interesting phenomena can be observed: first, some cubes in the sample have a concavity on each of their faces (marked with arrow 4, 5 in Fig. 3a); second, some of the cubes congregate with each other into a fishbone-like structure with length to 30 μm. Figs. 3b and c show two typical cuboidal microcrystals with different concave faces in the same samples, both of which have approximative edge lengths of about 2.0 μm.

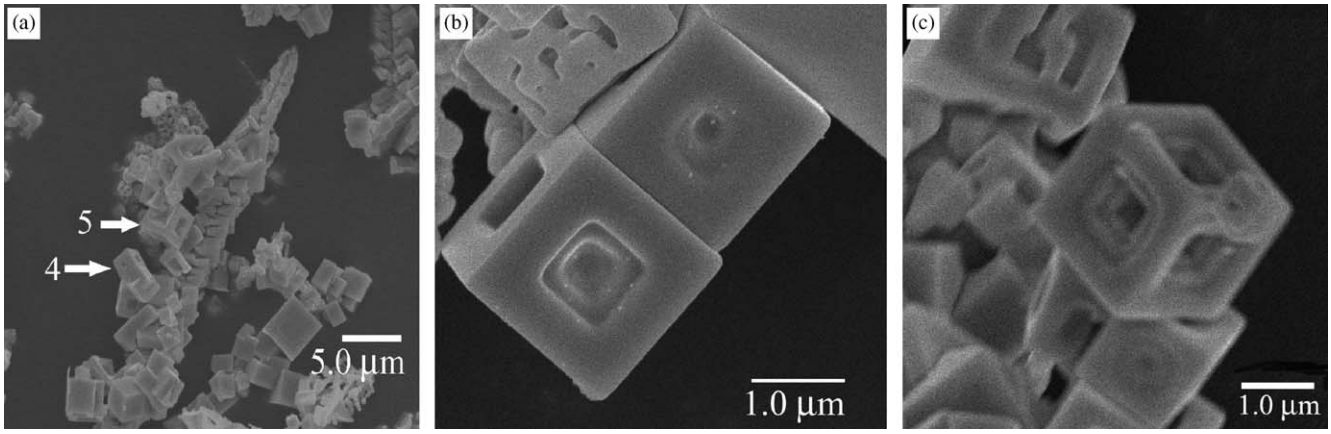

Fig. 3. SEM images of the cuboidal structures: (a) the panoramic image; (b–c) typical cuboidal structures with different concave faces.

3.4. Supplemental experiments for influence factors

To elucidate the relationship between reaction systems involved in the synthesis and the morphologies of the final products, we investigated the crystal growth under several different conditions. When the amount of glycerol added in the system was changed, there was little change in the morphologies of the products except that the small branches on each trunk of these multiple-dendritic hierarchical structures became less obvious, as shown in Fig. 4a, which indicates the ratio of glycerol and deionized water in the reaction system has little influence on the morphologies of the PbSe crystals. In addition, Fig. 4b shows the FESEM image of the sample prepared by the process without SDBS. Compared with Fig. 2a, besides the structurally 4-fold symmetrical multiple-dendritic hierarchical structures, there are some dendritic fractals (marked with arrow 2, 3, respectively, in Fig. 2e) similar to individual offshoot of the multiple-dendritic hierarchical structure, and it further confirms that the presence of SDBS in the reaction system is favorable for the growth of structurally 4-fold symmetrical multiple-dendritic framework.

The influence of the reaction temperature to the product morphologies in our experiments was not remarkable. At lower reaction temperature, the obtained products are well-crystalline PbSe multiple-dendritic hierarchical structures coexisting with some irregular nanoparticles. While at higher reaction temperatures, such as 160, 180 and 200 °C, the obtained products presented only uniform and well-crystalline PbSe multiple-dendritic hierarchical structures as shown in Fig. 2.

3.5. Possible formation mechanism

In both approaches to two kinds of structures, the formation of PbSe was based on the combination of Pb^{2+} and Se^{2-}. In the case of using SeO_2 as selenium source, Se^{2-} ions were produced as following equation, in which SeO_2 was dissolved in the alkaline solution to form SeO_3^{2-}

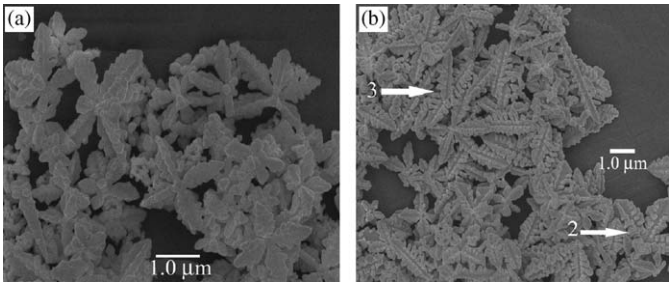

Fig. 4. (a) The sample obtained in the reaction system with 20 ml glycerol; (b) the sample prepared with out SDBS.

and then was reduced to Se^{2-} by the superfluous hydrazine.

$$2SeO_2 + 4OH^- \rightarrow 2H_2O + 2SeO_3^{2-} \xrightarrow{3N_2H_4} 3N_2 + 2Se^{2-} + 6H_2O. \quad (1)$$

In the case of using Se powders as selenium source, Se^{2-} ions were produced from the hydrolysis of Se powders, as illustrated below:

$$3Se + 6OH^- \rightarrow 2Se^{2-} + SeO_3^{2-} + 3H_2O. \quad (2)$$

In both reaction systems, glycerol acted as a complexing reagent to form the complex, $Pb(C_3H_6O_3)$, which sharply decreased the free Pb^{2+} concentration in the solution and slowed the speed of the following reaction for the formation of PbSe crystals:

$$Pb(C_3H_6O_3) + Se^{2-} \rightarrow PbSe + C_3H_6O_3. \quad (3)$$

It is well known that slow reaction rate is favorable for crystallization as well as the separation of the growth step and the nucleation step.

On the basis of our experiments, we assume the growth process of the two kinds of PbSe structures to be a nucleation-preferential growth process. The factors influencing the crystal growth involve kinetics and crystallography. It was concluded by Murphy [21] that the preferential absorption of molecules and ions in solution to different crystal faces directs the growth of nanoparticles into various shapes by controlling the growth rates along

different crystal axes. Wang [22] suggested that the shape of an fcc nanocrystal is mainly determined by the ratio of the growth rate in the ⟨100⟩ to that in the ⟨111⟩. Then, with respect to the structure of fcc PbSe, we speculate that these structures were formed in an analogous process. The growth scheme of the two kinds of PbSe structures is summarized in Scheme 1. In detail, when SeO_2 was used as selenium source and hydrous hydrazine as reducing reagent, once the PbSe nuclei are formed in the earlier stage of the reaction (3), these nuclei would preferentially grow along the ⟨111⟩ directions if new reactants are continuously arriving at the sites. Moreover, the different rates of adsorption and de-adsorption of SDBS ions on the different planes of PbSe nuclei would kinetically influence the growth rates of these planes, and, thus, the fast growth along eight ⟨111⟩ directions may be ascribed to the less adsorption of SDBS ions on (111) plane. As a result, continuous growth of PbSe in the ⟨111⟩ directions forms structurally symmetrical eight trunks of the hierarchical structure. Subsequent growth along another three crystallographically equivalent ⟨111⟩ directions around one trunk, as illuminated by the lattice (inset in Fig. 2b), in which one trunk of the dendrite grows along the ⟨111⟩ direction denoted by black line and the small branches grow along the three ⟨111⟩ directions denoted by black lines with white spots, leads to the formation of 3-fold symmetric branches on three sides of the trunk. The possible growth was further confirmed by TEM image and ED pattern in Fig. 2d.

Our results have shown that the process of obtaining PbSe multiple-dendritic hierarchical structure and cuboidal microcrystals mainly depended on the difference of the selenium sources. For synthesis of cuboidal structure of PbSe microcrystals, Se^{2-} ions were produced from the hydrolysis of the Se powders in alkaline solution as Eq. (2), which proceeded rather more slowly compared with that from reduction by hydrazine described in Eq. (1). The lower concentration of Se^{2-} in the reaction system leads to the slower growth of the PbSe crystal. It is well known that slow growing rate is favorable to form thermodynamically stable structure, and, thus, for PbSe unit, cube is the thermodynamically stable morphology of PbSe. However, on the other hand, the initial growth preferentially along ⟨111⟩ due to the presence of surfactants SDBS gave birth to some incomplete {100} faces in the cubes. Consequently, because of integrative contribution of the preferential growth along ⟨111⟩ due to the SDBS followed by the thermodynamically stable growth of {100} faces due to the slower growing rate, cuboidal structures were obtained in such a reaction system using Se powders as selenium source and in the absence of hydrous hydrazine.

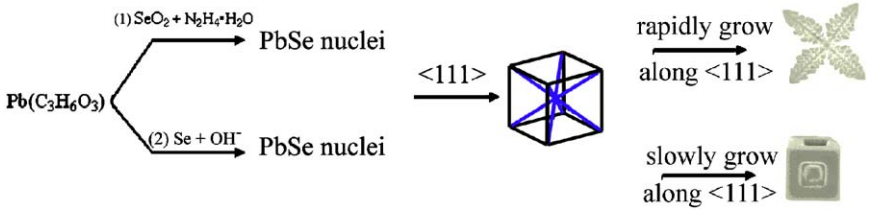

Scheme 1. Illustration of the formation process of two kinds of PbSe structures.

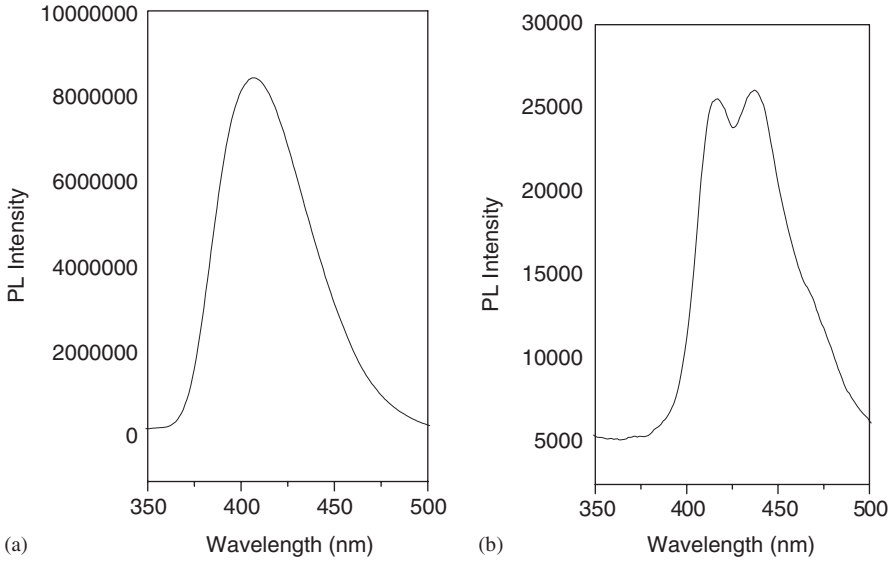

Fig. 5. Photoluminescence (PL) spectrum of (a) multiple-dendritic PbSe hierarchical structures and (b) cuboidal PbSe microcrystals.

3.6. Photoluminescence spectra of the products

To examine the PL properties of the products, the room-temperature PL spectra of the two kinds of PbSe microstructures were studied, in which the solid samples were characterized without any treatment. Figs. 5a and b depict, respectively, the PL emission spectra of the PbSe multiple-dendritic hierarchical structure and cuboidal microcrystals. Under PL excitation at 360 nm, the PL spectra in Figs. 5a and b display some differences. In Fig. 5a, a distinct emission peak is located at 407 nm which is due to the second excitonic transitions (el→hl) in PbSe nanocrystals [23]. In Fig. 5b, the top of the emission peak was separated into two peaks located, respectively, at 416 nm and 437 nm which may be corresponding to the second excitonic transitions (el→hl) and electronic transitions caused by defects in the interfacial region [24]. The PL spectra in Figs. 5a and b reveal that the peak position changed a little, while the intensity and shape changed in large degree. The characteristic differences of two PL spectra are mainly corresponding to the diversities in their shapes and defects in the interfacial region [24], which may be caused by different synthesis methods for the two samples. The separation of the emitting peaks in Fig. 5b may be attributed to the existence of the crystal imperfections, such as point defects, dislocations, and grain boundaries in the sample of the cuboidal microcrystals. The relative intensities of the emission peaks seem closely related to the surface/volume ratio. The multiple-dendritic hierarchical structures have the bigger surface/volume ratio, and the relative intensity of the peak is much higher. In contrast, the relative intensity of the emission peak for cuboidal structures, which have the smaller surface/volume ratio, is the lower. On all accounts, the variation of the structures and defects density of the samples might be responsible for the appearance of differences in the two PL spectra. These results could indicate that the special structures might have some significant influence on the optical properties of PbSe crystals, which could be adopted in fine-tuning the surface-defect-related optical properties of this material.

4. Conclusion

In summary, a selected-control solution-phase route was successfully introduced to synthesize well-crystalline 3D PbSe structures under hydrothermal condition. PbSe multiple-dendritic hierarchical structures and cuboidal microcrystals could be selectively obtained by using different selenium sources in the reaction systems. Based on the evidence of electron microscope images, the possible growth mechanisms for the two kinds of PbSe structures were discussed and the influence factors were also investigated. The optical properties of these hierarchical PbSe microcrystals differ from those of the bulk crystals, which could be related to their structural complexity and specialty. Further detailed characterization of this relationship is needed. Lead selenide has an important role as a functional material, and thus the rational design of its complex structures could be of significance in applications. This synthesis method has demonstrated that it is possible to design complex and hierarchical structures by a facile, mild solution approach, which could be extended to the morphogenesis of other inorganic crystals with complex forms.

Acknowledgments

Financial support from the National Natural Science Foundation of China and the Chinese Ministry of Education is gratefully acknowledged.

Appendix A. Supporting information

Supplementary data associated with this article can be found in the online version at doi:10.1016/j.jssc.2005.09.043.

Reference

[1] D.J. Milliron, S.M. Hughes, Y. Cui, et al., Nature 430 (2004) 190.
[2] L. Manna, D.J. Milliron, A. Meisel, et al., Nat. Mater. 2 (2003) 382.
[3] J. Hu, L.S. Li, W. Yang, L. Manna, L.W. Wang, A.P. Alivisatos, Science 292 (2001) 2060.
[4] Y.W. Jun, Y.Y. Jung, J. Cheon, J. Am. Chem. Soc. 124 (2002) 615.
[5] G.M. Whitesides, B. Grzybowski, Science 295 (2002) 2418.
[6] I. Lisiecki, P.A. Albouy, M.P. Pileni, Adv. Mater. 15 (2003) 712.
[7] T.A. Witten, L.M. Sander, Phys. Rev. Lett. 47 (1981) 351.
[8] P. Meakin, Phys. Rev. Lett. 51 (1983) 1119.
[9] D.B. Kuang, A.W. Xu, Y.P. Fang, H.Q. Liu, Adver. Mater. 15 (2003) 1747.
[10] S.H. Xie, W.Z. Zhou, Y.Q. Zhu, J. Phys. Chem. B 108 (2004) 11561.
[11] M.H. Cao, T.F. Liu, C.W. Hu, Z.L. Wang, Angew. Chem. Int. Ed. 44 (2005) 2.
[12] P.D. Yang, T. Deng, D.Y. Zhao, P.Y. Feng, D. Pine, B.F. Chmelka, G.M. Whitesides, G.D. Stucky, Science 282 (1998) 2244.
[13] P. Gadenne, Y. Yagil, G.J. Deutscher, Appl. Phys. 66 (1989) 3019.
[14] X.F. Liu, M.D. Zhang, Int. J. Infrared Millimeter Waves 21 (2000) 1697.
[15] P.A. Kondas, Report ARFSD-TD-92024 (1993).
[16] T.C. Harman, PCT International Application Wo. 9416465 (1994) (US Application, 93-2451121).
[17] J.J. Zhu, O. Palchik, A. Gedanken, J. Phys. Chem. B 104 (2000) 7344.
[18] J.J. Zhu, H. Wang, S. Xu, Langmuir 18 (2002) 3306.
[19] Y.F. Liu, J.B. Cao, S.Y. Zhang, Eur. J. Inorg. Chem. (2003) 644.
[20] W.Z. Wang, Y. Gen, Y.T. Qian, M.R. Ji, X.M. Liu, Adv. Mater. 10 (1998) 1479.
[21] C.J. Murphy, Science 298 (2002) 2139.
[22] Z.L. Wang, J. Phys. Chem. B 104 (2000) 1153.
[23] S. Guha, V.J. Leppert, S.H. Risbud, I. Kang, Solid State Commun. 105 (1998) 695.
[24] Q.W. Chen, D.L. Zhu, C. Zhu, J. Wang, Y.G. Zhang, Appl. Phys. Lett. 82 (2003) 1018.